

Constraints on Galactic Intermediate Mass Black Holes

M. Mapelli¹, A. Ferrara¹ & N. Rea²

¹*SISSA, International School for Advanced Studies, Via Beirut 4, 34100, Trieste, Italy; mapelli@sissa.it*

²*SRON, Netherlands Institute for Space Research, Sorbonnelaan, 2, 3584 CA, Utrecht, The Netherlands*

23 September 2018

ABSTRACT

Intermediate Mass Black Holes (IMBHs; $10^{1.3-5} M_{\odot}$) are thought to form as relics of Population III stars or from the runaway collapse of stars in young clusters; their number and very existence are uncertain. We ran N-body simulations of Galactic IMBHs, modelling them as a halo population distributed according to a Navarro, Frenk & White (NFW) or a more concentrated Diemand, Madau & Moore (DMM) density profile. As IMBHs pass through Galactic molecular/atomic hydrogen regions, they accrete gas, thus becoming X-ray sources. We constrain the density of Galactic IMBHs, Ω_{\bullet} , by comparing the distribution of simulated X-ray sources with the observed one. From the null detections of Milky Way Ultra-Luminous X-ray sources, and from a comparison of simulations with unidentified sources in the IBIS/ISGRI catalogue we find a strong upper limit $\Omega_{\bullet} \leq 10^{-2} \Omega_b (\leq 10^{-1} \Omega_b)$ for a DMM (NFW) profile, if IMBHs accrete via ADAF disks. Slightly stronger constraints ($\Omega_{\bullet} \leq 10^{-3} \Omega_b$ for a DMM profile; $\Omega_{\bullet} \leq 10^{-2} \Omega_b$ for a NFW profile) can be derived if IMBHs accrete with higher efficiency, such as by forming thin accretion disks. Although not very tight, such constraints are the most stringent ones derived so far in the literature.

Key words: black hole physics - methods: N-body simulations - Galaxy: general - X-rays: general

1 INTRODUCTION

There are strong observational evidences for the existence of two classes of black holes (BHs): stellar mass BHs, with mass from 3 to 20 M_{\odot} (Orosz 2003), thought to be the relics of massive stars, and super massive black holes (SMBHs) in the mass range $10^{6-9} M_{\odot}$, hosted in the nuclei of many galaxies. Recently, the existence of a third class of Intermediate Mass BHs (IMBHs) has been inferred. They are characterized by masses in the range from $20 M_{\odot}$ to a few $\times 10^4 M_{\odot}$ (see van der Marel 2004 for a review).

Several IMBH formation mechanisms have been proposed: (i) IMBHs could be the relics of very massive metal free stars (Heger & Woosley 2002), (ii) they could form in young clusters via runaway collapse of stars (Portegies Zwart & McMillan 2002), or (iii) could have been built up in globular clusters through repeated mergers of stellar mass BHs in binaries (Miller & Hamilton 2002). Some recent observations indicate that IMBHs could exist in the core of globular clusters (Gebhardt, Rich & Ho 2002, 2005; Gerssen et al. 2002; van den Bosch et al. 2005). Their number is nearly unknown. In principle, IMBHs could contribute to all the baryonic dark matter (van der Marel 2004): their density Ω_{\bullet} could be essentially equal to that of luminous baryonic matter, $\Omega_{b, lum} = 0.021$ (Persic & Salucci 1992;

Fukugita, Hogan & Peebles 1998), and equal to 50% of all baryons ($\Omega_b = 0.044$, Spergel et al. 2003). Only weak constraints on the IMBH mass have been inferred from dynamical studies of the Milky Way. For example, the observed velocity dispersion of stars in the Galactic disk requires that halo BHs masses are $\leq 3 \times 10^6 M_{\odot}$, if the Milky Way dark halo is entirely made of compact objects (Carr & Sakellariadou 1999; see also Lacey & Ostriker 1985; Wasserman & Salpeter 1994; Murali, Arras & Wasserman 2000 and reference herein). Other dynamical constraints on the IMBH mass can be derived by imposing that they do not disrupt too many Galactic globular clusters (Moore 1993; Arras & Wasserman 1999). By this request, Klessen & Burkert (1996) found that, if the dark halo of the Milky Way is exclusively composed by IMBHs, their mass must be $\leq 5 \times 10^4 M_{\odot}$. For the same reason, the halo BHs cannot represent more than 2.5-5 per cent of the dark halo mass, if they are as massive as $10^6 M_{\odot}$ (Murali et al. 2000). However, constraints on IMBHs obtained from globular cluster disruption are very uncertain, as we do not know what are the characteristics of globular clusters when they form, and how many of them have been destroyed. It could even be that IMBHs have played a role in determining the current number and distribution of globular clusters (Ostriker, Binney & Saha 1989).

In this paper we explore an alternative way to dynamical

ically constrain the IMBH density, based on the proposed identification of Ultra-Luminous X-ray sources (ULXs) with IMBHs. ULXs are, by definition, point sources with X-ray luminosity higher than 10^{39} erg s $^{-1}$, exceeding the isotropic Eddington limit for a $10 M_{\odot}$ BH (see Colbert & Miller 2005 for a review). ULXs have not been found, up to now, in the Milky Way; but they are present in many spiral and starburst galaxies (Swartz et al. 2004). ULXs tend to be associated with star forming regions; but they often lie near, not in them (Mushotzky 2004).

ULXs were initially identified with SMBHs with a low accretion rate; but this interpretation was found to be in conflict with their position in the host galaxies, far off from the galaxy center (Colbert & Miller 2005). Later on ULXs have been suggested to be high-mass X-ray binaries (HMXBs) with beamed X-ray emission (King et al. 2001; Grimm, Gilfanov & Sunyaev 2003; King 2003). Even though low luminosity ULXs ($L_X \lesssim 5 \times 10^{39}$ erg s $^{-1}$) are consistent with this HMXB scenario, the highest luminosity ULXs show various characteristics which can be hardly reconciled with the beaming model (Miller, Fabian & Miller 2004), such as the existence of a ionized nebula surrounding some bright ULXs (Pakull & Mirioni 2002; Kaaret, Ward & Zezas 2004).

An intriguing hypothesis, at least for these highest luminosity ULXs (Miller et al. 2004), is their identification with accreting IMBHs. This idea is also supported by some observational evidences. First, the spectra of many high luminosity ULXs have a soft component well fitted by a multicolor black-body disk, whose inner temperature is typical of BH masses in the IMBH range (Miller et al. 2004; Colbert & Miller 2005). In addition, high luminosity ULXs often show long term variability on timescales of months to years (Kaaret et al. 2001; Matsumoto et al. 2001; Miyaji, Lehmann & Hasinger 2001) and quasi periodic oscillations (Strohmayer & Mushotzky 2003), inconsistent with the beaming scenario. King & Dehnen (2005) propose that very high luminosity ULXs in interacting galaxies can be IMBHs hosted in the merging satellite and whose accretion is activated by tidal forces.

Many studies have been dedicated to check the possibility that ULXs are IMBHs accreting in binary systems (Baumgardt et al. 2004; Hopman, Portegies Zwart & Alexander 2004; Kalogera et al. 2004; Portegies Zwart, Dewi & Maccarone 2004; Hopman & Portegies Zwart 2005; Patruno et al. 2005). However, the observed population of ULXs is not well reproduced by this binary system scenario (Blecha et al. 2005; Madhusudhan et al. 2005), mainly because the ULX phase of simulated IMBHs is too short. A better agreement between simulations and observations can be obtained only by considering very massive IMBHs ($\gtrsim 1000 M_{\odot}$; Baumgardt et al. 2005). In addition, very few optical counterparts have been detected for ULXs so far and can unambiguously be identified as companion stars (Liu et al. 2005; Colbert & Miller 2005). Then, it is still open the possibility that ULXs are IMBHs accreting gas during the transit through a dense molecular cloud, as recently suggested by Krolik (2004) and by Mii & Totani (2005).

This paper is aimed at exploring in detail this last hypothesis by dedicated N-body simulations (Section 2). In particular, we simulate a Milky Way model and we derive an upper limit of the density of IMBHs, by requiring that no ULX is produced in the Milky Way by IMBHs passing

through molecular clouds (Section 3). Next, we study the distribution of both ULX and non-ULX sources produced by IMBHs passing through molecular clouds (Section 3) and atomic hydrogen regions (Section 4). We finally compare the derived distributions with observations (Section 5).

2 NUMERICAL SIMULATIONS

The simulations have been carried out using the parallel N-body code Gadget-2 (Springel 2005). The simulations were performed using 8 nodes of the 128 processor cluster *Avogadro* at the *Cilea* (<http://www.cilea.it>). Our aim is to generate a suitable N-body model of the Milky Way, in which we embed a halo population of IMBHs.

2.1 Milky Way model

To reproduce the Milky Way we simulated an exponential disk and a Hernquist spherical bulge, whose density profiles are given, respectively, by the following relations (Hernquist 1993):

$$\rho_d(R, z) = \frac{M_d}{4\pi R_d^2 z_0} \exp -(R/R_d) \operatorname{sech}^2(z/z_0) \quad (1)$$

$$\rho_b(r) = \frac{M_b a}{2\pi} \frac{1}{r(a+r)^3}, \quad (2)$$

where M_d (M_b) is the disk (bulge) mass, R_d is the disk scale radius, z_0 is the disk scale height, a is the bulge scale length and $r = \sqrt{R^2 + z^2}$. We choose $a = 0.2 R_d$, consistent with Kent, Dame & Fazio (1991; $a = 0.7 \pm 0.2$ kpc). The value of z_0 is quite difficult to constrain. Recent observations (Larsen & Humphreys 2003; Yoachim & Dalcanton 2005) suggest the presence of two components in the thin disk of the Milky Way: a "young star forming" thin disk (with scale height ~ 200 pc) and an "old" thin disk (with scale height ~ 600 pc). Then, we assume $z_0 = 0.1 R_d = 350$ pc, which is approximately an average of the scale height of these two components and correlates in a simple way with R_d .

Disk and bulge are embedded in a rigid dark matter halo, whose density profile is (Navarro, Frenk & White 1996, hereafter NFW; Moore et al. 1999):

$$\rho_h(r) = \frac{\rho_s}{(r/r_s)^\gamma [1 + (r/r_s)^\alpha]^{(\beta-\gamma)/\alpha}}, \quad (3)$$

where we choose $(\alpha, \beta, \gamma) = (1, 3, 1)$, and $\rho_s = \rho_{\text{crit}} \delta_c$, ρ_{crit} being the critical density of the Universe and

$$\delta_c = \frac{200}{3} \frac{c^3}{\ln(1+c) - (c/(1+c))}, \quad (4)$$

where c is the concentration parameter and r_s is the halo scale radius, defined by $r_s = R_{200}/c$; R_{200} is the radius encompassing a mean overdensity of 200 with respect to the background density of the Universe, i.e. the radius containing the virial mass M_{200} . Given the concentration c and the Hubble parameter¹ $H(z)$, R_{200} , M_{200} and the circular velocity at the virial radius, V_{200} , are related by the following

¹ We adopt $H(z \lesssim 1) = H_0 = 71$ km s $^{-1}$ Mpc $^{-1}$ in agreement with first year WMAP results (Spergel et al. 2003)

expressions.

$$R_{200} = \frac{V_{200}}{10 H(z)}$$

$$M_{200} = \frac{V_{200}^3}{10 G H(z)}; \quad (5)$$

G is the gravitational constant. In our simulations we fix $c = 12$, $V_{200} = 160 \text{ km s}^{-1}$ (see Klypin, Zhao & Somerville 2002), yielding $M_{200} = 1.34 \times 10^{12} M_{\odot}$, $R_{200} = 225 \text{ kpc}$ and $r_s = 19 \text{ kpc}$ (Table 1 reports the initial parameters); finally, we use for $H(z)$ its actual value H_0 .

Rigid halos can induce $m = 1$ instabilities in the disk. To check this effect, we performed test simulations with a non-rigid halo (with halo particles ten times more massive than disk particles); we did not observe significant differences in the evolution with respect to fixed-halo models. Since simulations with non-rigid halos are prohibitively time consuming for the very high resolutions required by the problem (see Section 2.3 for details), we have chosen to adopt a rigid halo.

To derive M_d , M_b and R_d we followed the prescriptions of Mo, Mao & White (1998), imposing that the disk is a thin, dynamically stable and centrifugally supported structure, whose mass is a fraction of the halo mass and whose angular momentum is a fraction of the halo angular momentum. In particular, our best, stable model is obtained for a choice of the spin parameter $\lambda = 0.035$, where $\lambda \equiv J|E|^{1/2}G^{-1}M^{-5/2}$ (J , E and M being the angular momentum, the total energy and the mass of the halo, respectively). Requiring that $M_d + M_b \approx 0.04 M$ and that $M_d : M_b = 4 : 1$ (in agreement with Kent et al. 1991; Freudenreich 1998; Binney & Merrifield 1998), we obtain $M_d = 4 \times 10^{10} M_{\odot}$ and $M_b = 1 \times 10^{10} M_{\odot}$. Our choices are in agreement both with the best model of Milky Way described in Klypin et al. (2002) and with the COBE measurements of the bulge mass ($M_b = 1.3 \pm 0.5 \times 10^{10} M_{\odot}$, Dwek et al. 1995). For these values, the scale radius of the disk is $R_d = 3.5 \text{ kpc}$, consistent with recent estimates (Binney & Merrifield 1998). Given the uncertainty on the M_d/M_b ratio, we also made some test simulations for $M_d : M_b = 5 : 1$ observing no significant differences in our results. In order to account for the SMBH in the nucleus of the Milky Way, we located a point mass $M_{SMBH} = 3.5 \times 10^6 M_{\odot}$ (Ghez et al. 2003; Shödel et al. 2003) at the center of the rigid halo.

Initial velocities of disk and bulge particles are simulated using the Gaussian approximation (Hernquist 1993) for dispersion velocities. This choice introduces a transient behavior, represented by outwards propagating rings of over-density from the warmer disk center, as it was already noted by Kuijken & Dubinsky 1995 (see also Kazantzidis, Magorrian & Moore 2004; Widrow & Dubinski 2005). In agreement with the findings of Kuijken & Dubinsky 1995, in the highest resolution runs (when the mass of each particle is $m \lesssim 10^5 M_{\odot}$ and the total number of particles approaches one million) this transient is stronger; nevertheless, it always disappears within about 1 timescale², when the system relaxes into a new equilibrium configuration. We consider this new relaxed configuration as initial condition for our analysis. This procedure is legitimate in our case, since we are not

Table 1. Initial parameters for the Milky Way model.

c	12
V_{200}	160 km s ⁻¹
M_{200}	1.34 × 10 ¹² M _⊙
R_{200}	225 kpc
λ	0.035
M_d/M_b	4
M_d	4 × 10 ¹⁰ M _⊙
M_b	10 ¹⁰ M _⊙
R_d	3.5 kpc
z_0	0.1 R_d
a	0.2 R_d

investigating processes such as disk instabilities, but we are only interested in the dynamical evolution of halo IMBHs. After relaxation, we continue the simulation for about 5 Gyr, i.e. from redshift $z \approx 0.5$ until today, about half of the time elapsed from the last major merger (Governato et al. 2004). This allows us to follow the evolution of an already relaxed and nearly unperturbed (by mergers) Milky Way. During the entire simulation disk and bulge remain perfectly stable.

2.2 Intermediate mass black holes

How many IMBHs are hosted in the Milky Way? What is their spatial distribution? These are yet unanswered questions. Nevertheless, we need an *Ansatz* on the IMBH number, mass and distribution to generate the initial conditions of our simulations. A reasonable estimate for the initial IMBH number follows from Volonteri, Haardt & Madau 2003. Assuming that the IMBHs are born in $\nu\sigma$ fluctuations (with $\nu = 3 - 3.5$) collapsing at a given redshift, Volonteri et al. (2003) derive the density of IMBHs at the formation redshift $\Omega_{\bullet,f}$ as

$$\Omega_{\bullet,f} = [1 - \text{erf}(\nu/\sqrt{2})] \Omega_M \frac{m_{\bullet,f}}{M(\nu)}, \quad (6)$$

where $[1 - \text{erf}(\nu/\sqrt{2})]\Omega_M$ is the fraction of the Universe matter in halos with $M > M(\nu)$ ($\Omega_M = 0.27$ being the matter density), as derived from the Press & Schechter (1974) formalism, and $m_{\bullet,f}/M(\nu)$ is the fraction of mass of the halo collapsed in IMBHs ($m_{\bullet,f}$ being the average initial IMBH mass, and $M(\nu)$ the mass of the $\nu\sigma$ peak halo). For example, assuming that IMBHs form in 3σ fluctuations collapsing at redshift $z = 24$, the corresponding halo mass is $M(3) = 1.7 \times 10^5 M_{\odot}$ (Barkana & Loeb 2001). Under these assumptions equation (6) gives $\Omega_{\bullet,f} = 10^{-4} \Omega_b (m_{\bullet,f}/10^3 M_{\odot})$.

Given $\Omega_{\bullet,f}$, one can roughly estimate the number of IMBHs in the Milky way, N_{\bullet} as

$$N_{\bullet} = \frac{\Omega_{\bullet,f} M_{b,MW}}{\Omega_b m_{\bullet,f}}, \quad (7)$$

where $M_{b,MW} = (0.5 - 1) \times 10^{11} M_{\odot}$ is the mass in baryons of the Milky Way. Adopting a value of $\Omega_{\bullet,f} = 10^{-4} \Omega_b$, we find $N_{\bullet} \approx 10^4$. Instead, if we assume that IMBHs form in 3.5σ fluctuations collapsing at $z = 24$, this number becomes $N_{\bullet} = 5 \times 10^2$. We will adopt equations (6) and (7) to calculate how many IMBHs to include in our simulations.

² The timescale of our simulation is defined as the rotation period of the simulated galaxy, i.e. about 0.27 Gyr.

How massive are the IMBHs today? We have assumed that their average mass at formation was $m_{\bullet,f} = 10^3 M_{\odot}$. However, it is likely that they accreted gas for some period of their life (Ricotti & Ostriker 2004; Madau et al. 2004; Shapiro 2005; Volonteri & Rees 2005). The duration and the efficiency of accretion are highly uncertain, making hard to determine the amount of accreted mass. Shapiro (2005) suggests that the IMBH mass evolution $m_{\bullet}(t)$, assuming Edington rate accretion, can be written as:

$$m_{\bullet}(t) = m_{\bullet,f} \exp\left(\frac{1-\epsilon}{\epsilon} \frac{t}{t_{Salp}}\right), \quad (8)$$

where ϵ is the radiative efficiency ($\epsilon \approx 0.1$) and t_{Salp} is the Salpeter time ($t_{Salp} \approx 0.45$ Gyr). In our case t is the fraction of IMBH life during which it accretes at the Edington rate, i.e. $t = f_{duty} t_{birth}$, where t_{birth} is the time elapsed from the IMBH formation (≈ 13.5 Gyr) and f_{duty} is the fraction of t_{birth} during which the IMBH accretes. Assuming $f_{duty} \approx 0.01$ ($f_{duty} \lesssim 0.03$ for quasars at $z \approx 6$, Steidel et al. 2002), we obtain $m_{\bullet}(t) \approx 10 m_{\bullet,f}$. For our choice of $m_{\bullet,f} = 10^3 M_{\odot}$, this means that the average mass of IMBHs today is $m_{\bullet}(t) \approx 10^4 M_{\odot}$, consistent with the value $1.8 \times 10^4 M_{\odot}$ of the recently detected IMBH candidate in the globular cluster G1 (Gebhardt et al. 2005) and with previous theoretical estimates (Volonteri et al. 2003). This estimate is affected by a number of uncertainties, and we consider it only as an educated guess.

Due to accretion, the current density of IMBHs Ω_{\bullet} will be

$$\Omega_{\bullet} = \frac{m_{\bullet}(t)}{m_{\bullet,f}} \Omega_{\bullet,f} \approx 10 \Omega_{\bullet,f} = 10^{-3} \Omega_b (m_{\bullet,f}/10^3 M_{\odot}), \quad (9)$$

our reference value.

We note that other models predict very different values for Ω_{\bullet} . For example, Salvaterra & Ferrara (2003) derived $\Omega_{\bullet} \approx 0.1 \Omega_b$, under the assumption that Population III stars are the sources of the observed near-infrared excess with respect to galaxy counts. One of the aims of this paper is to check which part of the Ω_{\bullet} range is allowed by the link between IMBHs and ULXs (see next section). For this reason, we also carried out two runs adopting the estimate by Salvaterra & Ferrara (2003).

The last problem we have to address is the selection of initial conditions for the position and velocity distribution of IMBHs. White & Springel (2000) suggested that remnants of Population III stars should be much rather concentrated inside present-day halos. N-body cosmological simulations by Diemand, Madau & Moore (2005, hereafter DMM) seem to support this idea; they also show that the present spatial distribution of objects formed in high- σ fluctuations depends only on the rarity of the peak in which they are born. In particular, DMM find that the spatial distribution, in present halos, of objects formed in a $\nu\sigma$ fluctuation is well fitted by a modified Navarro-Frenk-White profile:

$$\rho_{\bullet}(r) = \frac{\rho_s}{(r/r_{\nu})^{\gamma} (1 + (r/r_{\nu})^{\alpha})^{(\beta_{\nu}-\gamma)/\alpha}}, \quad (10)$$

where ρ_s , α and γ are the same as defined in the previous section; $r_{\nu} \equiv r_s/f_{\nu}$ is the scale radius for objects formed in a $\nu\sigma$ fluctuation (with $f_{\nu} = \exp(\nu/2)$), and $\beta_{\nu} = 3 + 0.26 \nu^{1.6}$. As DMM simulations are collisionless, they cannot take into account the possible formation of binaries containing IMBHs (eventually with the central SMBH) and the occurrence of

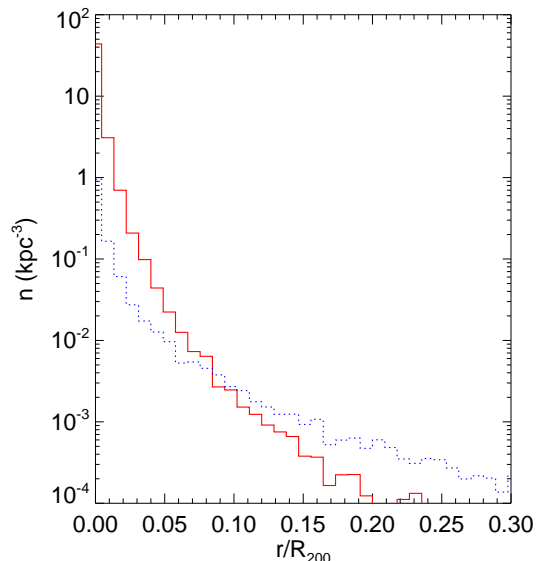


Figure 1. Density profile of IMBHs for a DMM (case A1; solid line) and for a NFW distribution (case A2; dotted line).

three-body encounters, which likely lead to the ejection of one of the involved IMBHs (Volonteri et al. 2003). Thus, the actual IMBH distribution could be slightly more “diluted” than that obtained by DMM.

2.3 Description of runs

We made three different sets of simulations, A, B and C, whose characteristics are described in Table 2. Simulations labeled as A are characterized by $\Omega_{\bullet} = 10^{-3} \Omega_b$ (corresponding to IMBHs formed in 3σ fluctuations), simulations B have $\Omega_{\bullet} = 10^{-1} \Omega_b$ (corresponding to the Salvaterra & Ferrara 2003 model), and the simulation C has $\Omega_{\bullet} = 3 \times 10^{-5} \Omega_b$ (corresponding to IMBHs formed in 3.5σ fluctuations). Simulations A1, B1 and C adopt the DMM spatial distribution, assuming that IMBHs form in 3σ (A1, B1) or 3.5σ (C) peaks. Instead, runs A2 and B2 were performed assuming that IMBHs follow a normal NFW profile. In Fig. 1 we compare the two considered distributions of IMBHs, i.e. DMM and NFW. In each simulation we evolved about 10^6 particles, each having a mass of $5 \times 10^4 M_{\odot}$ (included the IMBH particles). These particles are divided in $\approx 8 \times 10^5$ disk particles and $\approx 2 \times 10^5$ bulge particles, plus a variable number of IMBH particles: 2000 in each run of the group A (corresponding to 10^4 IMBHs of $10^4 M_{\odot}$; see equations (7) and (8)), 2×10^5 in each run of the group B (corresponding to 10^6 IMBHs of $10^4 M_{\odot}$) and 100 in the run C (corresponding to 500 IMBHs of $10^4 M_{\odot}$). CPU time limits require that we consider only equal mass particles, with mass no lower than $5 \times 10^4 M_{\odot}$ (included the IMBH particles), making impossible to investigate the impact of dynamical friction on the IMBH spatial distribution.

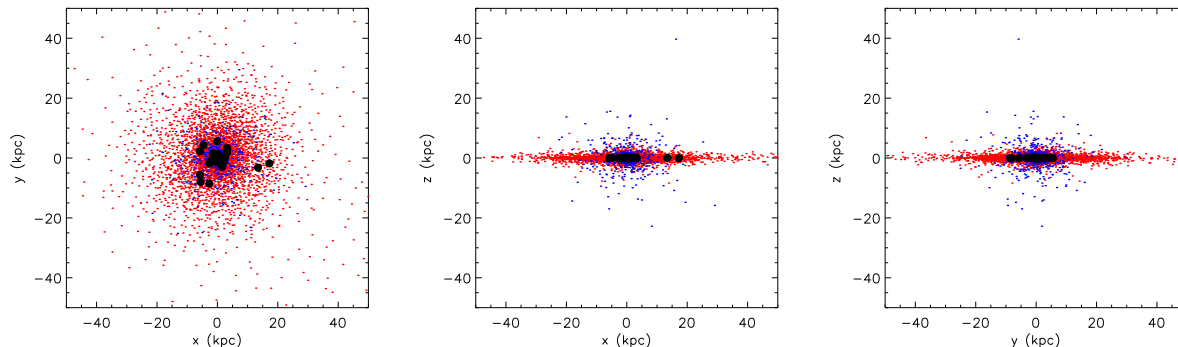


Figure 2. Snapshots at $t = 1.4$ Gyr (about 5 Galactic timescales) of the simulated Milky Way; only 1/200 of the total bulge and disk particles are plotted. Big dots indicate the IMBHs passing through the molecular disk in the case A1. Left panel: particle positions in the $x - y$ plane; central: in the $x - z$ plane; right: in the $y - z$ plane.

Table 2. Initial parameters for the IMBHs.

Run	Number of IMBH particles	$\Omega_{\bullet}/\Omega_b$	IMBH profile
A1	2000	10^{-3}	DMM ^a
A2	2000	10^{-3}	NFW ^b
B1	2×10^5	10^{-1}	DMM
B2	2×10^5	10^{-1}	NFW
C	100	3×10^{-5}	DMM

^aDiemand, Madau & Moore 2005.

^bNavarro, Frenk & White 1996.

3 IMBHs ACCRETING MOLECULAR GAS

As discussed in the Introduction, one of the possible explanations for the existence of ULXs is that they are IMBHs, accreting both in binary systems (Patruno et al. 2005) or in molecular clouds (Mii & Totani 2005). Here we investigate the possibility that ULXs are IMBHs accreting gas during their transit within a molecular cloud. We also checked how many non-ultra-luminous X-ray sources ($L_X < 10^{39}$ erg s^{-1}) could be produced by IMBHs passing through molecular clouds.

3.1 IMBH density constraints from ULXs

The X-ray luminosity³ of a BH with mass M_{\bullet} , expected from the Bondi-Hoyle accretion in a gas cloud, can be expressed as (Edgar 2004; Mii & Totani 2005):

³ More precisely, equation (11) refers to the bolometric luminosity due to the Bondi-Hoyle accretion. However, detailed models of spectra of black holes accreting in the Bondi-Hoyle regime (Beskin & Karpov 2005) or forming ADAF disks (Narayan, Mahadevan & Quataert 1998) show that more than 60% of the bolometric luminosity is emitted in the X-ray range and more than 40% between 0.2 and 10 keV (approximately the bandpass of Chandra and XMM). Because of the other uncertainties in our calculations, we think that the approximation that nearly all the Bondi-Hoyle luminosity is emitted in the X-ray band is acceptable.

$$L_X(\rho, v) = 4\pi\eta c^2 G^2 M_{\bullet}^2 \rho \tilde{v}^{-3}, \quad (11)$$

where η takes into account the radiative efficiency and the uncertainties in the accretion rate, c is the light speed, ρ the density of the molecular cloud and $\tilde{v} = (v^2 + \sigma_{MC}^2 + c_s^2)^{1/2}$, v being the IMBH velocity relative to the gas; σ_{MC} and c_s are the molecular cloud turbulent velocity and gas sound speed, respectively. Recently, Krumholz, McKee & Klein (2006) have shown that accretion rates in a turbulent medium might slightly differ from the above one. Because of the many uncertainties in our model, we do not attempt to deal with these subtleties. From equation (11) and following Agol & Kamionkowski (2002), Mii & Totani (2005) derive the number of ULXs with luminosity higher than L_X as⁴:

$$N_{ULX}(> L_X) \approx 2.2 \times 10^{-2} N_{\bullet} f_{disk} \mu^{-1} \eta \times \left(\frac{M_{\bullet}}{10^4 M_{\odot}} \right)^2 \left(\frac{10^{39} \text{ erg s}^{-1}}{L_X} \right), \quad (12)$$

where μ is the mean molecular weight ($\mu \approx 1.2-2.3$ depending on the fraction of H_2 molecules), N_{\bullet} is the number of IMBHs in the Milky Way (see equation 7) and η is the radiative efficiency. The correct value of η is completely uncertain. In fact, we do not even know whether an accretion disk forms at all. Agol & Kamionkowski (2002) show that most of BHs accreting gas should form accretion disks; but these disks are not necessarily thin. If the accreting gas is able to form a thin accretion disk (Shakura & Sunyaev 1974), then $\eta = 0.1$, as assumed by Mii & Totani (2005). However, it seems to be more realistic that the gas forms an ADAF (i.e. Advection-Dominated Accretion Flow) disk, whose radiative efficiency⁵ is of the order of $\eta = 0.001$ for IMBHs of mass $M_{\bullet} \sim 10^4 M_{\odot}$ (Quataert & Narayan 1999). Finally,

⁴ We consider only the particular case of the equation by Mii & Totani (2005) in which $M_{\bullet} \gtrsim 10^3 M_{\odot}$.

⁵ The luminosity for an ADAF disk scales as \dot{M}^2 , where \dot{M} is the accretion rate. However, if $\log(\dot{M}/\dot{M}_{Edd}) \sim -4, -2$, where \dot{M}_{Edd} is the Eddington accretion rate, the efficiency of an ADAF disk is about two orders of magnitude lower than the efficiency of a thin disk (see Figure 7 of Narayan et al. 1998). We can assume that the efficiency of an ADAF disk is $\eta = 10^{-3}$, because the accretion rates of the IMBHs we are considering fall in the range above.

models which take into account gas magnetization (Beskin & Karpov 2005) show that a high efficiency ($\eta \approx 0.1$) is allowed, even if the thin disk does not form. To decide among these different models is beyond the scope of this paper; we will consider the two different values $\eta = 0.1$ and $\eta = 0.001$ bracketing the above possibilities in all our cases.

In equation (12) f_{disk} is the fraction of IMBHs passing through the molecular disk of the Galaxy, for which we assume a scale height $z_{MC} = 75$ pc and a radial extension $R_{MC} \approx 20$ kpc (Sanders, Solomon & Scoville 1984). Mii & Totani estimated $f_{disk} \approx 4.5 \times 10^{-4}$, based on the hypothesis that IMBHs are a halo population following a standard NFW profile. Our simulations allow a more precise and direct estimate of f_{disk} from our simulations. As an example, in Fig. 2 we show a snapshot of our simulations, where the positions of IMBHs passing through the molecular disk are shown. Table 3 reports the simulated values for f_{disk} and N_{ULX} with luminosity $L_X \geq 10^{39}$ erg s $^{-1}$.

For $\eta = 0.1$, we find that, if IMBHs are born in 3σ fluctuations (corresponding to $\Omega_\bullet \approx 10^{-3}\Omega_b$) and their present distribution in the Milky Way follows the DMM model (case A1), the number of ULXs associated with these IMBHs is still consistent with zero ($N_{ULX} \approx 0.2$; Table 3, third column). Instead, if $\Omega_\bullet \approx 10^{-1}\Omega_b$ (case B1), the Milky Way should host about 30 active ULXs. Then, we conclude that, if the IMBHs follow a DMM distribution, $\Omega_\bullet \approx 10^{-3}\Omega_b$ can be considered as an upper limit for the present density of IMBHs. If, on the contrary, the IMBHs follow a standard NFW profile, as assumed by Mii & Totani (2005), the number of ULXs obtained for $\Omega_\bullet \approx 10^{-1}\Omega_b$ (case B2) is still marginally consistent with zero. Finally, if IMBHs follow the DMM distribution but form only in fluctuations with $\sigma \gtrsim 3.5$, they are so rare that no ULX is expected to be seen in the Milky Way (case C1).

However, if IMBHs are surrounded by low efficiency ADAF disks ($\eta = 10^{-3}$), the upper limit for a DMM profile becomes $\Omega_\bullet = 0.1\Omega_b$; whereas there are nearly no constraints for the NFW profile. It is worth noting that Mii & Totani (2005) mainly considered the case of maximal efficiency ($\eta = 0.1$), which is probably unlikely according to Agol & Kamionkowski (2002).

Equation 12 tells us even another information: the dark matter halo of the Milky Way cannot be entirely composed by BHs with mass $\gtrsim 10^5 M_\odot$. In fact, if $M_\bullet = 10^5 M_\odot$ and $N_\bullet = 10^7$ (corresponding to the assumption that the Milky Way dark matter halo is composed by BHs as massive as $10^5 M_\odot$), $N_{ULX}(> 10^{39} \text{ erg s}^{-1}) \sim 2 \times 10^5 \eta$ for a DMM profile and $N_{ULX}(> 10^{39} \text{ erg s}^{-1}) \sim 9 \times 10^3 \eta$ for a NFW model. This means $N_{ULX} \gg 1$ both for a thin and an ADAF disk model (unless $\eta \ll 10^{-3}$). Then, the dark matter halo can be entirely composed by BHs only if their mass is less than $10^5 M_\odot$, ruling out the scenario proposed by Lacey & Ostriker (1985), in which halo BHs can account for the galactic disk heating.

3.2 Radial and luminosity distribution of ULXs

The previous results can be refined by using our simulations instead of equation (12). In fact, from the simulations we know the number $N(z < z_{MC})$ of IMBH particles which at a given time are in the molecular disk (defined by the scale height $z_{MC} = 75$ pc and the radial extension

$R_{MC} \approx 20$ kpc). It is well known that H $_2$ in the Galaxy is not distributed uniformly within such disk, but it has a clumpy structure made of molecular clouds. Following Agol & Kamionkowski (2002) we derive the actual volume fraction of the molecular disk occupied by the clouds, i.e.

$$f_{MC} = \frac{(\beta - 2)\langle \Sigma_{MC} \rangle}{(\beta - 1)2\mu m_p z_{MC} n_{min}} \left[1 - \left(\frac{n_{max}}{n_{min}} \right)^{(1-\beta)} \right] \approx 0.017, \quad (13)$$

where $\beta = 2.8$ for an H $_2$ cloud, $\langle \Sigma_{MC} \rangle = 29 M_\odot \text{ pc}^{-2}$ (Sanders et al. 1984; Mii & Totani 2005) is the average surface density of molecular clouds, m_p is the proton mass, $n_{min} = 10^2 \text{ cm}^{-3}$ and $n_{max} = 10^5 \text{ cm}^{-3}$ are the minimum and maximum density, respectively, observed in molecular clouds. Thus, the number of IMBHs which at a given time t are embedded into a molecular cloud is $N(z < z_{MC})f_{MC}$. In practice, we randomly select from our simulations a fraction f_{MC} of the IMBHs which at a given time t have $z < z_{MC}$ and $R < R_{MC}$. For this sample of IMBHs, we derive the Bondi-Hoyle luminosity L_X as in equation (11), assuming that $c_s = 0.3 \text{ km s}^{-1}$ and $\sigma_{MC} = 3.7 \text{ km s}^{-1}$ (Larson 1981; Solomon et al. 1987; Mii & Totani 2005). We then identify as ULXs those IMBHs which have $L_X > 10^{39} \text{ erg s}^{-1}$. Averaging this number over the entire simulation, we obtain an estimate $\tilde{N}_{ULX}(> L_X)$ of the number of ULXs in the Milky Way. For all the considered cases, the number $\tilde{N}_{ULX}(> L_X)$ (Table 3, fourth column), derived in this way, is consistent with the value $N_{ULX}(> L_X)$ (Table 3, third column), derived from equation (12), confirming the validity of the Mii & Totani calculation.

This alternative method to derive the number of ULXs contains additional important pieces of information concerning the spatial distribution of ULXs and their luminosities (see Fig. 3 for the case B1). These distributions are meaningless for the Milky Way, where no ULXs have been detected. Nevertheless, it could be interesting to compare them with the distributions of ULXs observed in other spiral galaxies. Fig. 3 shows that, if a DMM profile is adopted for IMBHs, ULXs appear to be mostly concentrated towards the Galactic center. This seems to be at odds with observations, which have shown that ULXs of external galaxies tend to be preferentially located in spiral arms (Liu & Bregman 2005). We have to keep in mind, though, that the present calculation is based on the molecular hydrogen distribution of the Milky Way, which could be quite different from that of other galaxies hosting ULXs; the latter are often starbursting, very gas rich systems.

The predicted ULX luminosities (Fig. 3) are mostly in the range $1 - 5 \times 10^{39} \text{ erg s}^{-1}$ with only few sources showing luminosities higher than $10^{40} \text{ erg s}^{-1}$. This rapid falloff of the number of ULXs for increasing X-ray luminosities is consistent with observations (Grimm et al. 2003). On the contrary, simulations following the accretion of IMBHs in binary systems indicate a number of low luminosity ULXs which is only a factor ≈ 2 higher than the number of sources with $L_X > 10^{40} \text{ erg s}^{-1}$ (Madhusudhan et al. 2005). As a caveat, we recall that our calculations assume a Bondi-Hoyle luminosity, which might be a relatively oversimplified approximation.

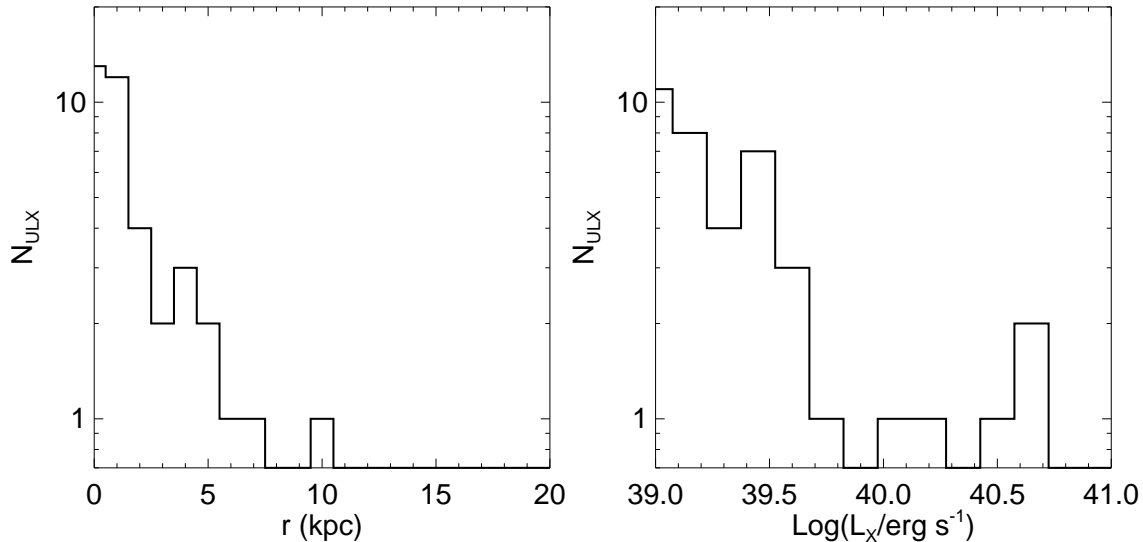


Figure 3. Distribution of ULXs as a function of their Galactocentric distance (left panel) and X-ray luminosity (right panel) for the case B1 and $\eta = 0.1$, after $\approx 0.5 Gyr$.

3.3 Non ULX sources

By using the technique described in Section 3.2, we can also derive the number of low luminosity X-ray (in brief, non-ULX) sources with $L_X < 10^{39}$ erg s $^{-1}$ (Table 3; fifth column). An interesting result is that, if $\eta = 0.1$, IMBH luminosities are always as high as 10^{37} erg s $^{-1}$ (see Fig. 4, where the dotted line represents IMBHs accreting molecular gas, including ULXs). Instead, if only ADAF disks can form, the luminosities reached by accreting IMBHs in molecular clouds are lower, in the range from 10^{35} to 10^{38} erg s $^{-1}$. Luminosities from 10^{37} to 10^{39} erg s $^{-1}$ are reached, in our Galaxy, only by a few supernova remnants (Vink 2006) and by high mass and low mass X-ray binaries (HMXBs, LMXBs; Psaltis 2006). Then, IMBHs accreting gas in molecular clouds should be among the most powerful Galactic X-ray sources and therefore should have been already detected, provided they are not transient. A strong constraint on the density of IMBHs thus descends from the requirement that the number of IMBHs with $L_X < 10^{39}$ erg s $^{-1}$ is lower than the number of detected Galactic sources emitting at the same luminosities which lack of certain identifications with other kind of objects (such as HMXBs and LMXBs). This analysis will be carried out in Section 5, considering X-ray sources produced by IMBHs accreting both within molecular clouds and atomic hydrogen regions.

4 IMBHs ACCRETING ATOMIC HYDROGEN

Mii & Totani (2005) neglected in their analysis IMBHs passing through atomic hydrogen regions, because their lower density ($\lesssim 1$ cm $^{-3}$) powers much lower X-ray luminosities than in molecular gas. (King et al. 2001). However, atomic hydrogen is much more diffuse in the Milky Way than H $_2$, and IMBHs are so massive that they can have non-negligible luminosity even accreting in such rarefied environment. Cur-

rent models of the hydrogen distribution in the Milky Way (McKee & Ostriker 1977; Rosen & Bregman 1995) suggest the existence of three different phases: a neutral cold component ($T \approx 10^2$ K), a warm ($T \approx 10^4$ K) and a hot ($T \approx 10^6$ K) component. In our work we neglect the hot component, since, even if its filling factor is high (up to 0.7, Rosen & Bregman 1995), it has an average density of $\approx 10^{-3}$ cm $^{-3}$ and a sound speed of ≈ 100 km s $^{-1}$, so that the X-ray luminosity of IMBHs accreting hot gas is expected to be very low. We define an atomic hydrogen disk as a disk having cut-off length $R_H = 20$ kpc (the data show an exponential fall of neutral hydrogen density outside 20 kpc; Lockman 2002) and scale height $z_H = 100$ pc (Baker & Burton 1975; Sanders et al. 1984; Dickey & Lockman 1990). Adopting the procedure described in Agol and Kamionkowski (2002), we derive the volume fraction occupied by cold neutral hydrogen, f_{CH} , as:

$$f_{CH} = \frac{(\beta_{CH} - 2)\langle \Sigma_{CH} \rangle}{(\beta_{CH} - 1)2\mu m_p z_H n_{min,CH}} \times \left[1 - \left(\frac{n_{max,CH}}{n_{min,CH}} \right)^{(1-\beta_{CH})} \right], \quad (14)$$

where $\beta_{CH} = 3.8$ (Agol & Kamionkowski 2002), $\langle \Sigma_{CH} \rangle$ is the average surface density of neutral hydrogen ($\langle \Sigma_{CH} \rangle = 4.5 M_\odot$ pc $^{-2}$ if $R > 4$ kpc and $\langle \Sigma_{CH} \rangle \approx 0$ if $R \leq 4$ kpc; Agol & Kamionkowski 2002; Sanders et al. 1984), $n_{min,CH}$ and $n_{max,CH}$ are the minimum and maximum density of neutral hydrogen, respectively ($n_{min,CH} \approx 1$ cm $^{-3}$, $n_{max,CH} \approx 5$ cm $^{-3}$; Bregman, Kelson & Ashe 1993). Substituting these values into equation (14), we obtain $f_{CH} = 0.48$ if $R > 4$ kpc and $f_{CH} \approx 0$ if $R \leq 4$ kpc. This value is in good agreement with run E of Rosen & Bregman (1995), which is a suitable fit of cold and warm hydrogen observations (Dickey & Lockman 1990). For consistency, we assume that the filling factor of the warm component is $f_{WH}=0.2$, as

Table 3. Results.

Run	f_{disk}^a	N_{ULX}^b	\tilde{N}_{ULX}^c	$N_{H_2}^d$	N_H^e	$N(10^{36-39} \text{ erg s}^{-1})^f$
A1	0.022±0.003	0.2 (0.002)	0.2±0.2 (0.002±0.002)	1.0±0.6 (1.2±0.5)	45±12 (45±12)	18±7 (1.2±1.0)
A2	0.0008±0.0006	0.008 (8×10^{-5})	0±0 (0±0)	0±0 (0±0)	5±4 (5±4)	0.4±0.4 (0±0)
B1	0.025±0.002	28 (0.28)	40±6 (0.5±0.5)	310±24 (350±24)	4056±125 (4058±125)	1650±70 (236±15)
B2	0.00090±0.00007	1 (0.01)	0.5±0.5 (0.007±0.007)	5.6±1.5 (6.1±1.5)	495±39 (495±39)	148±21 (5±3)
C	0.039±0.018	0.02 (0.0002)	0±0 (0±0)	0±0 (0±0)	3±3 (3±3)	0.09±0.09 (0±0)

The values refer to a thin disk with $\eta = 0.1$ (the values in parenthesis refer to an ADAF disk with $\eta = 0.001$).

^a Average fraction of IMBHs passing through the molecular disk (see Section 3.1).

^b Number of ULXs with $L_X \geq 10^{39} \text{ erg s}^{-1}$ derived from equation (12) adopting $\mu = 2$ (see Section 3.1).

^c Number of ULXs with $L_X \geq 10^{39} \text{ erg s}^{-1}$ derived from our simulations (see Section 3.2 and Fig. 3).

^d Number of sources which accrete molecular hydrogen (see Section 3.3) with X-ray luminosities $L_X < 10^{39} \text{ erg s}^{-1}$, derived from our simulations (see Fig. 4 and 5).

^e Number of sources which accrete atomic hydrogen (see Section 4), derived from our simulations. All of them have $L_X \leq 10^{39} \text{ erg s}^{-1}$ (see Fig. 4 and 5).

^f Number of sources which accrete atomic or molecular hydrogen and have X-ray luminosity $10^{36} \leq L_X < 10^{39} \text{ erg s}^{-1}$ (see Section 5).

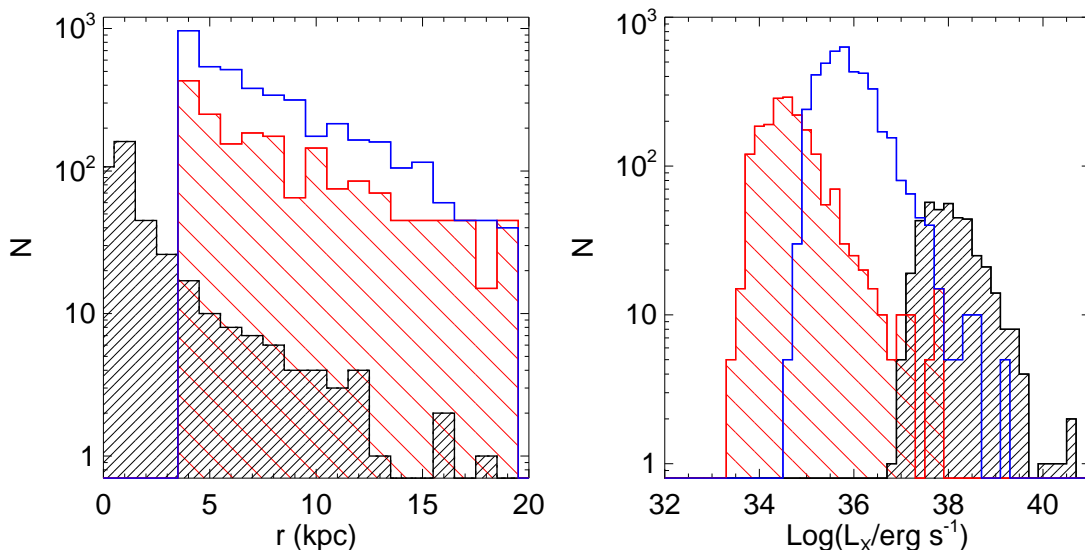


Figure 4. Distribution of all the X-ray sources as a function of the radial distance (left panel) and luminosity (right panel) for the case B1 and $\eta = 0.1$, after 2 timescales. Open histogram: IMBHs passing through cold neutral hydrogen; light shaded histogram: IMBHs passing through warm hydrogen; heavy shaded histogram: IMBHs passing through molecular hydrogen. Although the distributions slightly change with time due to the small statistics, their main features remain unaltered.

in run E of Rosen & Bregman (1995). Then, the number of IMBHs which, at a given time t , are passing through cold (warm) hydrogen regions is $N(z < z_H) f_{CH}$ ($N(z < z_H) f_{WH}$). Adopting the same procedure as in Section 3.2, we randomly select a fraction f_{CH} (for cold hydrogen) or f_{WH} (for warm hydrogen) of the IMBHs which, at a given time, pass through the neutral hydrogen disk, and we derive the Bondi-Hoyle luminosity⁶ for each of them using equation

(11). The results are shown in Table 3, sixth column, and in Figure 4.

If $\eta = 0.1$, IMBHs passing through cold neutral hydrogen regions show luminosities of the order of $10^{35-37} \text{ erg s}^{-1}$, with a high luminosity tail at $> 10^{38} \text{ erg s}^{-1}$; IMBHs passing through warm hydrogen regions produce lower luminosities, ranking from 10^{33} to $10^{35} \text{ erg s}^{-1}$ with an extended high luminosity tail extending to $10^{38} \text{ erg s}^{-1}$ (Fig. 4). Due to the large filling factor of the atomic hydrogen with respect to the molecular one, the number of IMBHs accreting HI is a factor $\approx 10 - 30$ higher than the number of IMBHs which accrete H_2 , even if the luminosities are lower and nearly no ULX can be produced in atomic regions.

⁶ We assume a turbulent velocity $\sigma_H = 10 \text{ km s}^{-1}$ both for cold and warm hydrogen (Lockman & Gehman 1991). The adopted sound speed is 1 km s^{-1} for cold hydrogen and 10 km s^{-1} for warm hydrogen regions.

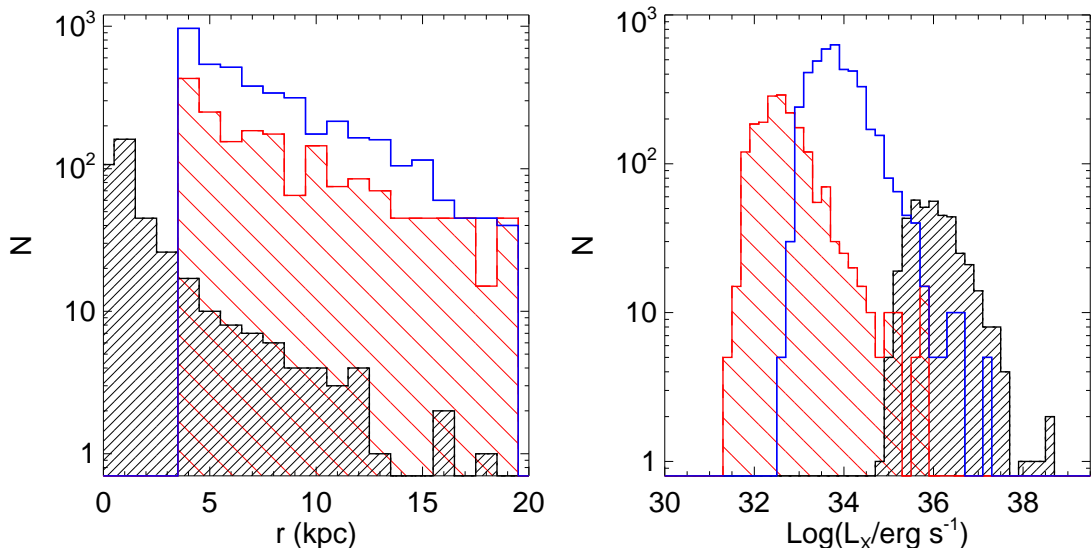


Figure 5. Distribution of all the X-ray sources as a function of their Galactocentric distance (left panel) and luminosity (right panel) for the case B1 and $\eta = 0.001$, after ≈ 0.5 Gyr. Open histogram: IMBHs passing through cold neutral hydrogen; light shaded histogram: IMBHs passing through warm hydrogen; heavy shaded histogram: IMBHs passing through molecular hydrogen. Although the distributions slightly change with time due to the small statistics, their main features remain unaltered.

Most interestingly, we note from the column 6 of Table 3 that for $\Omega_{\bullet} = 0.1 \Omega_b$ (both for $\eta = 0.1$ and for $\eta = 0.001$), the expected number of X-ray sources is huge, both for in the case of a DMM profile (case B1, ≈ 4000 sources) and for a NFW profile (case B2, ≈ 500 sources). The reason the case B2 (which yielded the acceptable number of ULXs ≈ 1) predicts so many X-ray sources depends on the HI distribution properties: atomic gas is less concentrated than molecular clouds. Because a number of X-ray sources (not identified with HMXBs or LMXBs) > 500 is definitely too high for the Milky Way, we can robustly exclude $\Omega_{\bullet} \gtrsim 0.1 \Omega_b$.

For $\eta = 0.001$, such as for an ADAF disk, IMBH luminosities are much lower, spanning 10^{31-35} to 10^{37} erg s $^{-1}$ (Fig. 5). Even if the total number of sources remains nearly unmodified (Table 3; sixth column), the fact that most of them present luminosities $\ll 10^{37}$ erg s $^{-1}$ makes comparison with observations more difficult. In the next section we attempt to constrain the Galactic IMBH density by comparison with X-ray observations, considering X-ray sources produced collectively by IMBHs accreting both within molecular clouds and atomic regions.

5 COMPARISON WITH OBSERVATIONS

In the previous Sections (3.1-3.2) we tried to constrain the density of IMBHs in our Galaxy by the fact that no ULXs have been detected in the Milky Way. From our simulations we found that some accreting IMBHs might also emit as non-ultraluminous X-ray sources, being in some cases bright enough to had been reliably detected by current X-ray satellites.

Hereafter, we match the results of our simulations with the X-ray observations. In particular, we compare the predicted IMBH X-ray emission with our knowledge of the X-

ray sky in order to define an upper limit on the presence of these objects in our Galaxy.

So far we have predicted IMBH X-ray luminosities (for a summary see Table 3) of $\approx 10^{31-39}$ erg s $^{-1}$, mostly depending on the assumed accretion efficiency η , disk model and molecular or atomic accreting material. Searching in the observations for an upper limit of possible IMBHs in such a wide luminosity range is a non-sense, mainly because at the low luminosities many sources were certainly missed.

What we then study here are only the IMBHs with a predicted hard X-ray luminosity between $10^{36} - 10^{39}$ erg s $^{-1}$ (see Table 3, last column). In all these cases, the high luminosity of these sources makes us confident that we should have seen them in the monitoring campaign of the Galaxy with the new generation satellites (within a certain distance depending of the flux resolution of the given satellite).

The most uncertain point is whether IMBHs accreting gas are transient or persistent sources. If the IMBH would be able to form a (thin or ADAF) accretion disk, it should also be a transient source. Instead, IMBHs accreting in the Bondi-Hoyle regime without forming a disk, as suggested by Beskin & Karpov (2005), should show flares; it remains unclear if they can be transient sources or not. On the other hand, the IMBH could be transient also as a consequence of properties of the interstellar medium. In fact the accretion rate is roughly proportional to the density of the gas, and the scintillation measures show that the density fluctuations of the interstellar medium can be as high as a factor 100 on scales from $\approx 10^{18}$ down to $\approx 10^{12}$ cm (Rickett 1990; Lambert & Rickett 2000; Cordes & Lazio 2001; Ferrara & Perna 2001). A halo IMBH can easily travel $\approx 10^{12}$ cm in about one day, and thus could suffer, in principle, changes of a factor ≈ 100 in its flux in this range of time. As a consequence,

we have considered all the sources meeting our requirements, both persistent or transient during the observations.

The most wide and sensitive survey available for our aims is the soft gamma-ray survey recently obtained by the IBIS/ISGRI (Imager on Board INTEGRAL Satellite/INTEGRAL Soft Gamma-Ray Imager) instrument on board of the INTEGRAL satellite (Bird et al. 2004, 2006). This survey observed 50% of the sky with a flux limit of 1 mCrab in the 20–100 keV energy range.

Among more than 200 sources detected by the IBIS/ISGRI soft gamma-ray survey scan, we excluded all the sources that certainly could not belong to the sample of possible IMBHs. In particular, we excluded all the well established X-ray binaries, which are a well known highly luminous Galactic class (both as transient and persistent sources). Furthermore we withdraw from our sample all the X-ray binaries known to host a neutron star (e.g. either because showing pulsations or thermonuclear bursts). We then filtered for a couple of highly energetic supernova remnants. After this first filtering we end up with a few tens of unknown objects.

Given the fact that what IBIS/ISGRI measures is a certain flux at Earth and not a luminosity, which is usually hard to derive because of the poorly known distances, we put the sample of sources we derived after the latter filtering, at distances between 1–15 kpc, and we took all the sources with an inferred luminosity $10^{36} - 10^{39} \text{ erg s}^{-1}$, which implies in terms of flux all the uncatalogued IBIS/ISGRI objects with a detected flux (within their errors) >4.8 mCrab in the 20–40 keV energy range. Note that this flux limit is derived placing a source emitting $10^{36} \text{ erg s}^{-1}$ at 15 kpc (e.g. the edge of our Galaxy), it would be detected by IBIS/ISGRI at a flux of 4.8 mCrab in the 20–40 keV energy range, well above the flux limit of the survey. Hence we are confident that, if present, our putative Galactic IMBHs would had been detected in the 50% of the Galaxy covered by the IBIS/ISGRI survey. Note that the flux limit of 4.8 mCrab we assumed includes, for the completeness of our analysis, the worst case of the faintest source at the largest distance: the fact that we are looking for an upper limit on the number of these possible IMBHs allow us to make this assumption.

Under these assumptions, we found only 3 IBIS/ISGRI unidentified sources which match our requirements. These sources were all persistent during the IBIS observations. Their luminosity falls in the 10^{36} - $10^{39} \text{ erg s}^{-1}$ range, all of them close to the $10^{36} \text{ erg s}^{-1}$ bound. As the IBIS/ISGRI catalogue covers 50% of the Galaxy, we then tentatively predict an upper limit of 6 sources with these characteristics in the entire Galaxy, if the volume observed is a fair sample. In a few years all the Galaxy will be covered by the IBIS/ISGRI survey and our tentative extrapolation may be refined.

Let us now compare this number with that of IMBHs predicted by our simulations in the same luminosity range and reported in the last column of Table 3.

a) *Thin disks*

For a thin disk, even case A1 ($\Omega_{\bullet} = 0.001 \Omega_b$, DMM profile) yields ≈ 18 sources, a value three times higher than observed. Furthermore, 4 of these simulated sources have $L_X > 10^{37} \text{ erg s}^{-1}$. From an additional run with $\Omega_{\bullet} = 10^{-4} \Omega_b$ and the DMM profile (not reported in Table 3 for simplicity) we saw that the number of sources with $10^{36} <$

$L_X < 10^{39} \text{ erg s}^{-1}$ is 0.6 ± 0.6 . We conclude that the upper limit in the case of a Shakura-Sunyaev disk and a DMM profile is $\Omega_{\bullet} = 10^{-4} - 10^{-3} \Omega_b$, similar to the upper limit found by the number of ULXs alone (see Section 3.1-3.2). Instead, for a NFW profile the allowed density of IMBHs is $> \Omega_{\bullet} = 10^{-3} \Omega_b$ (case A2; corresponding to 0.4 ± 0.4 sources), but definitely $< \Omega_{\bullet} = 10^{-1} \Omega_b$ (case B2; 148 ± 21 expected sources), strengthening the constraint we found from the number of ULX.

b) *ADAF disks*

For the more realistic case of an ADAF disk, the constraints we obtain from the comparison with the IBIS/ISGRI sources are stronger than for the number of ULXs alone. In fact, if we assume a DDM profile, the upper limit for the density of IMBHs is about $\Omega_{\bullet} = 10^{-3} \Omega_b$ (case A1; 1.2 ± 1.0 expected sources), much lower than $\Omega_{\bullet} = 10^{-1} \Omega_b$ (case B1; 236 ± 15 expected sources), derived from the number of ULXs. If we consider a NFW model, the upper limit is $\Omega_{\bullet} = 10^{-1} \Omega_b$ (case B2; 5 ± 3 expected sources); whereas there were no significant constraints from the ULXs. In summary, we must take with care the results of this comparison between simulated and observed X-ray sources, because of the huge uncertainties of our model. However, from the comparison with the IBIS/ISGRI unidentified sources we derive, in general, much stronger constraints than from the number of ULXs.

6 CONCLUSIONS

In this paper we have simulated the dynamical and emission properties of putative IMBHs which could inhabit our Galaxy. IMBHs are modeled as a halo population, distributed following a NFW or a more concentrated DMM profile. We assumed that IMBHs, passing through molecular or atomic hydrogen regions, could accrete gas, forming X-ray sources (either ultra-luminous or not). From the comparison of our simulations with the number of ULXs in the Galaxy (Section 3.1-3.2) and with the non-ultraluminous unidentified X-ray sources in the IBIS/ISGRI catalogue, we have derived the most stringent (to our knowledge) upper limits on the density Ω_{\bullet} of IMBHs. The main results can be summarized as follows:

- If IMBHs accrete with efficiency $\eta = 0.001$ (i.e. via an ADAF disk), we obtain a strong upper limit $\Omega_{\bullet} < 10^{-2} \Omega_b$ for a DMM profile and $\Omega_{\bullet} = 10^{-1} \Omega_b$ for a NFW profile.
- If the IMBHs accrete with efficiency $\eta = 0.1$ (i.e. if a thin accretion disk around the IMBH is formed), the upper limit of the density of IMBHs is $\Omega_{\bullet} = 10^{-3} \Omega_b$ for a DMM profile and $\Omega_{\bullet} = 10^{-2} \Omega_b$ for a NFW profile.

These results are still affected by some model uncertainties, as the emission mechanism and the IMBH distribution. In addition, computational requirements have forced us to use high and equal mass ($m_{\bullet} = 5 \times 10^4 M_{\odot}$) IMBH particles. Constraints for lower IMBHs masses are expected to be weaker. We can guess how the above upper limits change for different values of the IMBH mass by using the equation (12). For example, if we assume $m_{\bullet} = 10^3 M_{\odot}$, $\eta = 0.1$ and a DMM profile, the upper limit of the IMBH density becomes $\Omega_{\bullet} = 10^{-2} \Omega_b$, about one order of magnitude lower than for $m_{\bullet} = 10^4 M_{\odot}$. As a further caveat, this extension to

lower masses is possible only for the comparison with ULXs (and not with IBIS/ISGRI sources), because it is based on eq. (12). Therefore, higher resolution simulations would be required to extend our studies to lower mass IMBHs or to consider a more realistic IMBH mass spectrum. Higher resolution simulations (where the mass of star particles can be orders of magnitude lower than the mass of IMBH particles) are also needed to take into account the dynamical friction, which could play a crucial role.

Another caveat concerns the validity of the DMM profile. The simulations by DMM neglect the contribution of IMBHs in building up SMBHs, either by mergers (Islam, Taylor, & Silk 2003, 2004a,b,c) or by accretion and close dynamical encounters (Volonteri et al. 2003). Monte Carlo simulations combined with semi-analytical models (Volonteri & Perna 2005) show that, if all these factors are taken into account, the number of IMBHs could be up to 2 orders of magnitude lower, leading to an $\Omega_{\bullet} \sim 10 - 100$ lower than our estimates, and therefore compatible with the non-detection of ULXs in the Milky Way. However DMM take into account the bias in the formation sites of IMBHs, the accretion into larger halos, the role of both dynamical friction and tidal stripping, which were neglected or described by rough models in the previous studies. Unfortunately current simulations cannot account for all these effects at the same time. In conclusions, even if our results could be improved under many aspects, we consider it as a success that our models strengthen by a factor 10-1000 the currently adopted upper limits for the density of IMBHs (i.e. $\Omega_{\bullet} \approx 0.02$; van der Marel 2004).

ACKNOWLEDGEMENTS

We thank E. Ripamonti, L. Mayer, A. Possenti, M. Colpi, T. Maccarone, T. Di Salvo, L. Giordano, S. Callegari and C. Vignali for useful discussions and we acknowledge the Referee, Marta Volonteri, for her critical reading the manuscript. NR thanks R. Turolla and P. Jonker for useful discussion. We also thank A. Bazzano, L. Bassani e L. Kuiper for informations about the IBIS/ISGRI survey. We acknowledge for technical support the staff at *Cilea* and the system managers of the Kapteyn Institute of Groningen.

REFERENCES

- Agol E., Kamionkowski M., 2002, MNRAS, 334, 553
 Arras P., Wasserman I., 1999, MNRAS, 306, 257
 Baker P. L., Burton W. B., 1975, ApJ, 198, 281
 Barkana R., Loeb A., 2001, PhR, 349, 125
 Baumgardt H., Hopman C., Portegies Zwart S., Makino J., 2005, submitted to MNRAS, astro-ph/0511752
 Baumgardt H., Portegies Zwart S. F., McMillan S. L. W., Makino J., Ebisuzaki T., 2004, ASP Conf. Ser. 322: The Formation and Evolution of Massive Young Star Clusters, 322, 459
 Beskin G. M., Karpov S. V., 2005, A&A, 440, 223
 Binney J., Merrifield M., 1998, *Galactic astronomy*, Princeton University Press
 Bird A. J. et al. 2004, ApJL, 607, 33
 Bird A. J. et al. 2006, 2006, ApJ, 636, 765
 Blecha L., Ivanova N., Kalogera V., Belczynski K., Fregeau J., Rasio F., 2005, submitted to ApJ, astro-ph/0508597
 Bregman J. N., Kelson D. D., Ashe G. A., 1993, ApJ, 409, 682
 Carr B. J., Sakellariadou M., 1999, ApJ, 516, 195
 Colbert E. J. M., Miller M. C., 2005, Invited review talk at the Tenth Marcel Grossmann Meeting on General Relativity, Rio de Janeiro, July 20-26, 2003. Proceedings edited by M. Novello, S. Perez-Bergliaffa and R. Ruffini, World Scientific, Singapore, 2005
 Cordes J. M., Lazio T. J. W., 2001, ApJ, 549, 997
 Davies R. E., Pringle J. E., 1980, MNRAS, 191, 599
 Dickey J. M., Lockman F. J., 1990, ARA&A, 28, 215
 Diemand J., Madau P., Moore B., 2005, MNRAS, 364, 367 (DMM)
 Dwek E., Arendt R. G., Hauser M. G., Kelsall T., Lisse C. M., Moseley, S. H., Silverberg R. F., Sodroski T. J., Weiland J. L., 1995, ApJ, 445, 716
 Edgar R., 2004, NewAR, 48, 843
 Ferrara A., Perna R., 2001, MNRAS, 325, 1643
 Freudenreich H. T., 1998, ApJ, 492, 495
 Fujita Y., Inoue S., Nakamura T., Manmoto T., Nakamura K. E., 1998, ApJL, 495, 85
 Fukugita M., Hogan C. J., Peebles P. J. E. Peebles, 1998, ApJ, 503, 518
 Gebhardt K., Rich R. M., Ho L. C., 2002, ApJL, 578, 41
 Gebhardt K., Rich R. M., Ho L. C., 2005, ApJ, 634, 1093
 Gerssen J., van der Marel R. P., Gebhardt K., Guhathakurta P., Peterson R. C., Pryor C., 2002, AJ, 124, 3270
 Ghez A. M. et al., 2003, ApJL, 586, 127
 Governato F., Mayer L., Wadsley J., Gardner J. P., Willman B., Hayashi E., Quinn T., Stadel J., Lake G., 2004, ApJ, 607, 688
 Grimm H., Gilfanov M., Sunyaev R., 2003, MNRAS, 339, 793
 Heger A., Woosley S. E., 2002, ApJ, 567, 532
 Hernquist L., 1993, ApJS, 86, 389
 Hopman C., Portegies Zwart S. F., 2005, MNRAS, 363L, 56
 Hopman C., Portegies Zwart S. F., Alexander T. 2004, ApJL, 604, 101
 Islam R. R., Taylor J. E., Silk J., 2003, MNRAS, 340, 647
 Islam R. R., Taylor J. E., Silk J., 2004a, MNRAS, 354, 427
 Islam R. R., Taylor J. E., Silk J., 2004b, MNRAS, 354, 443
 Islam R. R., Taylor J. E., Silk J., 2004c, MNRAS, 354, 629
 Kalogera V., Henninger M., Ivanova N., King A. R. 2004, ApJL, 603, 41
 Kaaret P., Prestwich A. H., Zezas A., Murray S. S., Kim D.-W., Kilgard R. E., Schlegel E. M., Ward M. J., 2001, MNRAS, 321L, 29
 Kaaret P., Ward M. J., Zezas A., 2004, MNRAS, 351L, 83
 Kazantzidis S., Magorrian J., Moore B., 2004, ApJ, 601, 37
 Kent S. M., Dame T. M., Fazio G., 1991, ApJ, 378, 131
 King A. R., 2003, to appear in 'Compact Stellar X-Ray Sources', eds. W.H.G. Lewin and M. van der Klis, Cambridge University Press, astro-ph/0301118
 King A. R., Davies M. B., Ward M. J., Fabbiano G., Elvis M., 2001, ApJL, 552, 109
 King A. R., Dehnen W., 2005, MNRAS, 357, 275
 Klessen R., Burkert A., 1996, MNRAS, 280, 735
 Klypin A., Zhao Hs., Somerville R. S., 2002, ApJ, 573, 597
 Krolik J. H., 2004, ApJ, 615, 383
 Krumholz M. R., McKee C. F., Klein R. I., 2006, ApJ, 638, 369
 Kuijken K., Dubinski J., 1995, MNRAS, 277, 1341
 Lacey C. G., Ostriker J. P., 1985, ApJ, 299, 633
 Lambert H. C., Rickett B. J., 2000, ApJ, 531, 883
 Larsen J. A., Humphreys R. M., 2003, AJ, 125, 1958
 Larson R. B., 1981, MNRAS, 194, 809
 Liu J.-F., Bregman J. N., 2005, ApJS, 157, 59
 Liu J.-F., Bregman J. N., Seitzer P., Irwin J., 2005, astro-ph/0501310
 Lockman F. J., Gehman C. S., 1991, ApJ, 382, 182
 Lockman F. J., 2002, Seeing Through the Dust: The Detection of HI and the Exploration of the ISM in Galaxies, ASP Con-

- ference Proceedings, 276, 107. Edited by A. R. Taylor, T. L. Landecker, and A. G. Willis
- Madau P., Rees M. J., Volonteri M., Haardt F., Oh S. P., 2004, *ApJ*, 604, 484
- Madhusudhan N., Justham S., Nelson L., Paxton B., Pfahl E., Podsiadlowski Ph., Rappaport S., submitted to *ApJ*, astro-ph/0511393
- Matsumoto H., Tsuru T. G., Koyama K., Awaki H., Canizares C. R., Kawai N., Matsushita S., Kawabe R., 2001, *ApJL*, 547, 25
- McKee C. F., Ostriker J. P., 1977, *ApJ*, 218, 148
- Mii H., Totani T., 2005, *ApJ*, 628, 873
- Miller J. M., Fabian A. C., Miller M. C., 2004, *ApJL*, 614, 117
- Miller M. C., Hamilton D. P., 2002, *MNRAS*, 330, 232
- Miyaji T., Lehmann I., Hasinger G., 2001, *AJ*, 121, 3041
- Mo H. J., Mao S., White S. D. M., 1998, *MNRAS*, 295, 319
- Moore B., 1993, *ApJL*, 413, 93
- Moore B., Quinn T., Governato F., Stadel J., Lake G., 1999, *MNRAS*, 310, 1147
- Murali C., Arras P., Wasserman I., 2000, *MNRAS*, 313, 87
- Mushotzky R., 2004, *Progress of Theoretical Physics Supplement*, 155, 27
- Narayan R., Mahadevan R., Quataert E., 1998, *Theory of Black Hole Accretion Disks*, edited by Abramowicz M. A., Bjornsson G., and Pringle J. E.. Cambridge University Press, 148
- Navarro J. F., Frenk C. S., White S. D. M., 1996, *ApJ*, 462, 563 (NFW)
- Orosz J. A., 2003, *A Massive Star Odyssey: From Main Sequence to Supernova*, Proceedings of IAU Symposium 212, held 24-28 June 2001 in Lanzarote, Canary island, Spain. Edited by van der Hucht K. A., Herrero A., and Esteban C.. San Francisco: Astronomical Society of the Pacific, 365
- Ostriker J. P., Binney J., Saha P., 1989, *MNRAS*, 241, 849
- Pakull M. W., Mirioni L., 2003, *Winds, Bubbles, and Explosions: a conference to honor John Dyson*, Pátzcuaro, Michoacán, México, September 9-13 (Eds. S. J. Arthur & W. J. Henney), *Revista Mexicana de Astronomía y Astrofísica (Serie de Conferencias)*, 15, 197
- Patruno A., Colpi M., Faulkner A., Possenti A., 2005, *MNRAS*, 364, 344
- Persic M., Salucci P., 1992, *MNRAS*, 258P, 14
- Portegies Zwart S. F., Dewi J., Maccarone T., 2004, *MNRAS*, 355, 413
- Portegies Zwart S. F., McMillan S. L. W., 2002, *ApJ*, 576, 899
- Press W. H., Schechter P., 1974, *ApJ*, 187, 425
- Psaltis, D., 2006, To appear in "Compact Stellar X-ray Sources", eds. W.H.G. Lewin and M. van der Klis, astro-ph/0410536
- Quataert E., Narayan R., 1999, *ApJ*, 520, 298
- Rickett B. J., 1990, *ARA&A*, 28, 561
- Ricotti M., Ostriker J. P., 2004, *MNRAS*, 352, 547
- Rosen A., Bregman J. N., 1995, *ApJ*, 440, 634
- Salvaterra R., Ferrara A., 2003, *MNRAS*, 339, 973
- Sanders D. B., Solomon P. M., Scoville N. Z., 1984, *ApJ*, 276, 182
- Shakura N. I., Sunyaev, 1973, *A&A*, 24, 337
- Shapiro S. L., 2005, *ApJ*, 620, 59
- Shödel R., Ott T., Genzel R., Eckart A., Mouawad N., Alexander T., 2003, *ApJ*, 596, 1015
- Solomon P. M., Rivolo A. R., Barrett J., Yahil A., 1987, *ApJ*, 319, 730
- Spergel D. N., 2003, *ApJS*, 148, 175
- Springel V., 2005, *MNRAS*, 364, 1105
- Steidel C. C., Hunt M. P., Shapley A. E., Adelberger K. L., Pettini M., Dickinson M., Giavalisco M., 2002, *ApJ*, 576, 653
- Strohmayer T. E., Mushotzky R. F., 2003, *ApJL*, 586, 61
- Swartz D. A., Ghosh K. K., Tennant A. F., Wu K., 2004, *ApJS*, 154, 519
- van den Bosch R., de Zeeuw T., Gebhardt K., Noyola E., van de Ven G., 2005, accepted for publication in *ApJ*, astro-ph/0512503
- van der Marel R. P., 2004, *Coevolution of Black Holes and Galaxies*, from the Carnegie Observatories Centennial Symposia. Published by Cambridge University Press, as part of the Carnegie Observatories Astrophysics Series. Edited by L. C. Ho, 37
- Vink, J., 2006, to be published in the proceedings of the Symposium 'The X-ray Universe' 2005, astro-ph/0601131
- Volonteri M., Haardt F., Madau P., 2003, *ApJ*, 582, 559
- Volonteri M., Perna R., 2005, *MNRAS*, 358, 913
- Volonteri M., Rees M. J., 2005, *ApJ*, 633, 624
- Wasserman I., Salpeter E. E., 1994, *ApJ*, 433, 670
- White S. D. M., Springel V., 2000, *Proceedings of the MPA/ESO Workshop held at Garching, Germany, 4-6 August 1999*, 327, astro-ph/9911378
- Widrow L. M., Dubinski J., 2005, *ApJ*, 631, 838
- Yoachim P., Dalcanton J. J., 2005, *ApJ*, 624, 701